Local structure of the lead-free relaxor ferroelectric $(K_xNa_{1-x})_{0.5}Bi_{0.5}TiO_3$

V. A. Shuvaeva, D. Zekria, and A. M. Glazer
Clarendon Laboratory, Oxford University, Parks Road, Oxford OX1 3PU, United Kingdom

Q. Jiang, S. M. Weber, P. Bhattacharya, and P. A. Thomas
Department of Physics, University of Warwick, Coventry CV4 7AL, United Kingdom
(Received 28 April 2004; revised manuscript received 7 December 2004; published 27 May 2005)

The local environment of Bi and Ti atoms in the lead-free relaxor ferroelectric solid-solution $(K_xNa_{1-x})_{0.5}Bi_{0.5}TiO_3$ has been studied as a function of K concentration and as a function of temperature for the $x=0$ end member by x-ray absorption fine structure (XAFS). It is found that the local environment of Bi is much more distorted than that determined from conventional diffraction experiments. The shortest Bi-O distances are determined to be 2.22 Å, and are 0.3 Å shorter than those calculated from the crystallographic data. Several possible models of the Bi coordination environment, which are consistent with the XAFS data and provide bond-valence sums for Bi that are closer to the theoretical values, are proposed. The Ti displacement from the center of the oxygen octahedron increases with K concentration while the shortest Bi-O distance shows no compositional dependence. In $K_{0.5}Bi_{0.5}TiO_3$ the value of the Ti displacement is determined to be 0.18 Å. The changes of the macroscopic symmetry at the phase transition points in $Na_{0.5}Bi_{0.5}TiO_3$ do not lead to changes of the radial atomic distribution around Ti, which is well off-center over the whole temperature range up to and including the paraelectric cubic phase. The results can be explained by assuming the presence of structural disorder.

DOI: 10.1103/PhysRevB.71.174114 PACS number(s): 61.10.Ht, 77.84.Dy, 61.66.Fn, 61.50.Ks

I. INTRODUCTION

The origin of relaxor behavior in mixed-ion perovskites is of considerable current interest[1–3] and progress in this area relies on accurate information on the local and long-range crystal structure which, in turn, makes it possible to determine the values and orientation of local dipole moments. Obtaining such information is a challenging problem, as one has to characterize both structural and compositional disorder, which is found to be an intrinsic feature of relaxor perovskites. Diffraction methods, although the most powerful means for characterization of the long-range component of the structure of materials, are often relatively insensitive to local irregular deviations of atomic positions from the average ones.

X-ray absorption fine structure (XAFS) spectroscopy is one of the few techniques that provide direct quantitative information on the local structure in terms of the distribution of electron density around atoms of a selected type. The values of the displacements of transition metal atoms from sites of high symmetry can be determined both from extended x-ray absorption fine structure (EXAFS) and near-edge structure of the absorption spectra, which are known to be independent and sensitive probes.[4,5] Although the information about interatomic distances given by XAFS is usually not sufficient for constructing the whole structural model, it often provides valuable information about the structural peculiarities and allows one to verify a structural model. Application of these tools to the study of ferroelectric compounds has provided information on their structure and its thermal and compositional variation[6–11] which can assist in achieving a better understanding of the mechanisms of the phase transitions in these compounds. Previous XAFS investigations of phase transitions in a number of relaxor perovskite ferroelectrics[11] have shown that changes of macroscopic symmetry have surprisingly little effect on the local environment of atoms and that the local structure remains highly distorted even in the cubic phase.

Technological interest in $Na_{0.5}Bi_{0.5}TiO_3$ (NBT), $K_{0.5}Bi_{0.5}TiO_3$ (KBT), their solid solutions, and doped derivatives[12–26] has been driven by the fact that these particular relaxor ferroelectrics are among the few that do not contain lead atoms, making them suitable for the next-generation of environmentally friendly lead-free piezoelectrics. Of more fundamental interest is the fact that NBT and its analogs are compounds that have mixed-valency ions of very different electronic structure (e.g, Na and Bi) sharing the perovskite A site. The requirement to accommodate both Na^+ and Bi^{3+}, which is a lone-pair ion, on the shared A site gives rise to a sequence of interesting and unusual phase transitions and structures with both temperature and pressure.[27–30] In $Na_{0.5}Bi_{0.5}TiO_3$ rhombohedral, tetragonal, and cubic phases have been recorded with an intermediate mixed phase between rhombohedral and tetragonal, phases.[13–22] Two tetragonal ferroelectric phases at ambient and intermediate temperatures and the high-temperature cubic paraelectric phase have been found in $K_{0.5}Bi_{0.5}TiO_3$.[12,22,23] At room temperature, the macroscopic symmetry of the solid solutions of $(K_xNa_{1-x})_{0.5}Bi_{0.5}TiO_3$ (KNBT) changes from rhombohedral to tetragonal at about $x=0.25$ with increase of K concentration, as revealed by optical investigations and diffraction measurements.[23,24]

Structural disorder has been found to be an intrinsic feature of Pb-based relaxors.[31–34] However, in the KNBT system no structural disorder has been reported so far, although the average structure of different phases is well established by now[15–17] and the diffraction data along with the diffuse scattering found in NBT[25] contain strong indications of both

structural disorder and of a local environment for Bi that is very different from the average crystallographic one.

We report here the results of an XAFS study of the values of the relative atomic displacements in $(K_xNa_{1-x})_{0.5}Bi_{0.5}TiO_3$ and their changes with temperature and concentration. The purpose of examining the local environments of the atoms using a probe such as XAFS is to elucidate how this difficult and atypical accommodation of dissimilar A-site cations within the perovskite framework is accomplished. Following on from this, it is then possible to examine how the sequence of phase transitions is driven by local structure rather than longer-range interactions. The relationship between the macroscopic and the local symmetries is the focus of the present work.

II. EXPERIMENT

Both ceramics and crystals of KNBT were used in this study. 3N grade chemicals K_2CO_3, Na_2CO_3, Bi_2O_3 and TiO_2 were weighed to form $x=0$, 0.17, 0.22, 0.35, 0.5, 0.75, and 1. The mixtures were ground and mixed using ball milling in methanol for 24 h, dried, and pressed into disks. These were heated in a Pt crucible to 950 °C at a rate of 100 °C/h and left for 24 h before being cooled naturally to room temperature. For crystal growth, the chemicals were melted at ~1300 °C and held at this temperature for ~4 h before cooling at 3–5 °C/h to ~850 °C, and at 30 °C/h to room temperature. Finally, the solidified material in the crucible was knocked out carefully using a plastic rod. Powders for EXAFS experiments were produced by grinding the disks or crystals.

The x-ray diffraction patterns obtained from all the materials were consistent with the perovskite structure and did not show the presence of any additional phases. The single-crystal samples contained less potassium than in the starting composition, and so the actual composition of the crystals was determined via electron-probe microanalysis (EPMA) using a JEOL JXA-8600.

XAFS measurements were carried out at both the Bi L_{III} and Ti K absorption edges; for the Ti edge spectra were recorded in both the near-edge and the extended energy spectral regions. The samples of $(K_xNa_{1-x})_{0.5}Bi_{0.5}TiO_3$ were pellets, obtained by mixing carefully ground powders with appropriate amounts of boron nitride. Single crystals and powder samples of $PbTiO_3$, which was used as a reference compound, were also measured.

Measurements at the Bi L_{III} edge were performed in transmission at the Synchrotron Radiation Source (SRS) (Daresbury) operating at 2 GeV with current varying from 125 to 250 mA at beamline 9.2, which is equipped with a Si(220) double-crystal monochromator. Harmonic rejection was achieved by setting the double-crystal monochromator to the half-peak-intensity position. The beam intensity before and after the samples was measured using gas-filled ionization chambers. Room-temperature fluorescent Ti K-edge spectra (4.500 keV) were measured at ID26 of the European Synchrotron Radiation Facility (ESRF) operating at 6 GeV and 200 mA. The synchrotron radiation was focused by three mechanically independent undulators and monochromatized by a cryogenically cooled fixed-exit double-crystal Si(111) monochromator. The temperature-dependent Ti K-edge spectra of NBT were taken at beamline 7.1 of SRS equipped with a simple, harmonic-rejecting double-crystal Si(111) monochromator. A Ge x-ray detector array was used to count the fluorescence output. The surface of the sample was oriented at approximately 45° to the incident x-ray beam and the detector. The temperature of the sample was controlled and monitored to within an accuracy of ±1 K. The XANES region was measured using steps of 0.1–0.5 eV, while the XAFS region was scanned so as to obtain a step in k space smaller than 0.05 Å^2, and the acquisition time was 1 s per point. From 2 to 5 scans were collected to improve the signal-to-noise ratio. Since the compositional dependence of KNBT XAFS (ESRF ID26) and temperature-dependent NBT XAFS (SRS 7.1) have been measured under different experimental conditions they were analyzed separately and no direct quantitative comparison between these sets of spectra were made. The measured XAFS data were analyzed using the Viper and UWXAFS packages.[35–38]

The influence of self-absorption on the fluorescence Ti spectra was evaluated using the formula: $K=1+\mu_{abs}/(\mu_{background}+\mu_{fluor})$ (where $\mu_{background}$ is the absorption of the nonresonant atoms in the material and μ_{fluor} is the total absorption of the material at the fluorescent energy of the absorbing atom) and the corresponding corrections have been applied.

All the spectra were normalized and the XAFS signal $\chi(k)$ was obtained by subtraction of the atomic background $\mu_0(k)$ from the raw data $\mu(k)$. The extracted Ti K-edge and Bi L_{III}-edge XAFS of NBT are shown in Fig. 1. k^2-weighted $\chi(k)$ was then Fourier transformed to R space. The Fourier transformation was made over the k range 3–13.5 Å^{-1} at both the Bi L_{III} edge and the Ti K edge. A simulation of all possible single and multiple scattering contributions was made using the FEFF 8.20 code.[39] The structural data for NBT[15] was used in the ATOMS program[37] to prepare input for FEFF. In the fit of Bi-O, Bi-Ti, and Ti-O peaks only single scattering was taken into account as its input was the major contribution. A fit to the experimental XAFS was performed in the R distance range 1.2–3.2 Å for the Bi L_{III} edge and 1–2.1 Å for the Ti K edge.

III. RESULTS AND DISCUSSION

A. Bi L_{III}-XAFS

According to the structural model of the rhombohedral phase of NBT the Bi cations are located on the threefold axis.[15,16] The Bi nearest-neighbor environment, as calculated from the diffraction data, consists of four oxygen shells each formed by three oxygen atoms with radii equal to 2.51, 2.61, 2.91, and 2.99 Å. In the high-temperature tetragonal phase of NBT, Bi-O distances calculated from the structural parameters[17] vary in the range 2.64–2.88 Å. A similar Bi coordination is obtained from diffraction measurements for the tetragonal phase of KBT where the range of the distances is 2.60–2.99 Å.[22] Thus, in all the phases the shortest Bi-O distance is estimated to be more than 2.5 Å. However, such

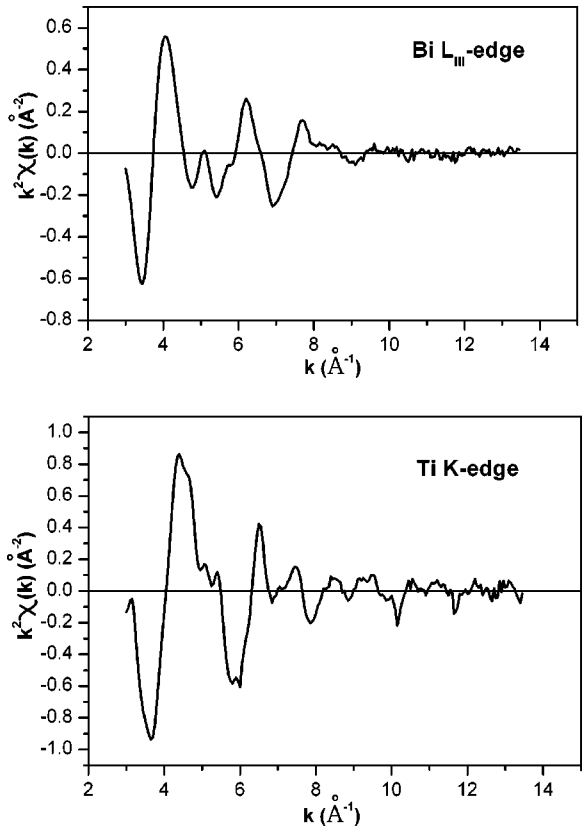

FIG. 1. k^2-weighted Bi L_{III}-edge and Ti K-edge EXAFS of NBT.

coordination is not typical for Bi^{3+} which tends to form much shorter Bi-O bonds. That this coordination did not satisfy the bond valence of Bi was noted[15,17,24] and the suggestion was made that the local structure of Bi should be different from the apparent structure that could be refined from the neutron diffraction data. In most bismuth oxides, including a number of perovskite compounds, where Bi usually occupies the B site, these distances vary in the range 2.2–2.3 Å.[40] Therefore, the large A site that it is occupying here is apparently not an ideal environment for it.

The longer-than-expected Bi-O distances obtained for KNBT from neutron diffraction experiments may originate from the inaccuracy of the average Bi position resulting from the presence of Bi disorder. Additional support for this assumption is provided by the large, highly anisotropic and sometimes even negative atomic displacement parameters of atoms, given by the refinement of the neutron diffraction powder data,[22] which are often indicative of structural disorder.

The Fourier transform (FT) of Bi L_{III}-XAFS for $Na_{0.5}Bi_{0.5}TiO_3$, shown in Fig. 2 by the dotted curve, has two major peaks, which can be attributed to the shortest Bi-O and Bi-Ti distances. No other peaks corresponding to Bi-O pairs are observed, which is probably due to a very broad distribution of longer Bi-O distances. In the same figure, the theoretical spectrum calculated on the basis of the x-ray diffraction data is presented. The shortest Bi-O and Bi-Ti distances were included in the calculations. Debye-Waller factors were chosen to obtain close values of the peak amplitudes in the experimental and calculated FT. It can be seen that the curves have a similar general profile, but the experimental FT XAFS peaks corresponding to Bi-O and Bi-Ti distances are located at much lower R compared with those for the calculated curve: this means that the real local distances in the compound are much shorter than those given by diffraction.

The fit to the XAFS data was made in the R range 1.2–3.2 Å, which corresponds to the first two peaks of the experimental FT XAFS. The XAFS fitting procedure imposes a limitation on the number of structural parameters involved in the refinement, which should not exceed the number of independent points defined by the formula $N_I = (2\Delta k \Delta r)/\pi + 2$. In the fitting procedure, the distance (R), the Debye-Waller factor (σ^2), the coordination number (N), and energy shift (ΔE_0) values were allowed to refine for each of the two coordination shells. Thus the total number of the refined parameters was 8 while the number of independent points in the fitted region was 14.

The best fit for NBT shown in Fig. 2(b) was obtained assuming that the first peak originated from one Bi-O shell and the second from one Bi-Ti shell. Attempts to include other Bi-O and Ti-O distances in the calculations resulted in significantly poorer fits. This shows that only a limited number of the shortest Bi-O and Bi-Ti distances are involved in the formation of the XAFS signal, while the contribution of other scattering processes is negligible. This may be due to the relatively broad distribution and significant variations of the longer Bi-O distances over the volume of the sample, which are probably highly affected by the local composition and particular distribution of Bi, K, and Na atoms over neighboring A sites. It should be noted that the peaks in the FT XAFS may originate not from one but from several shells which have close radii and thus are not resolved. High σ^2

TABLE I. Results of the fits to the XAFS data showing the distance (R), number of neighbors (N), the Debye-Waller factor (σ^2), and energy shift (ΔE_0) for the Bi-O and Bi-Ti shells in $(Na_{1-x}K_x)_{0.5}Bi_{0.5}TiO_3$.

	Bi-O shell				Bi-Ti shell				
x	R (Å)	N	σ^2 (Å^2)	E_0 (eV)	R (Å)	N	σ^2 (Å^2)	E_0 (eV)	R factor (%)
0	2.22(1)	4.0(6)	0.015(3)	−4(2)	3.21(2)	6(1)	0.025(5)	−4(1)	9.23
0.2	2.21(1)	3.2(7)	0.010(3)	−3(2)	3.20(2)	3(1)	0.015(5)	−4(2)	9.89
0.5	2.22(1)	3.2(6)	0.010(3)	−1(1)	3.22(2)	2.4(9)	0.010(4)	−2(1)	9.31
0.75	2.22(1)	3.1(5)	0.009(2)	−0(1)	3.24(2)	2.6(8)	0.009(4)	−0(1)	8.25

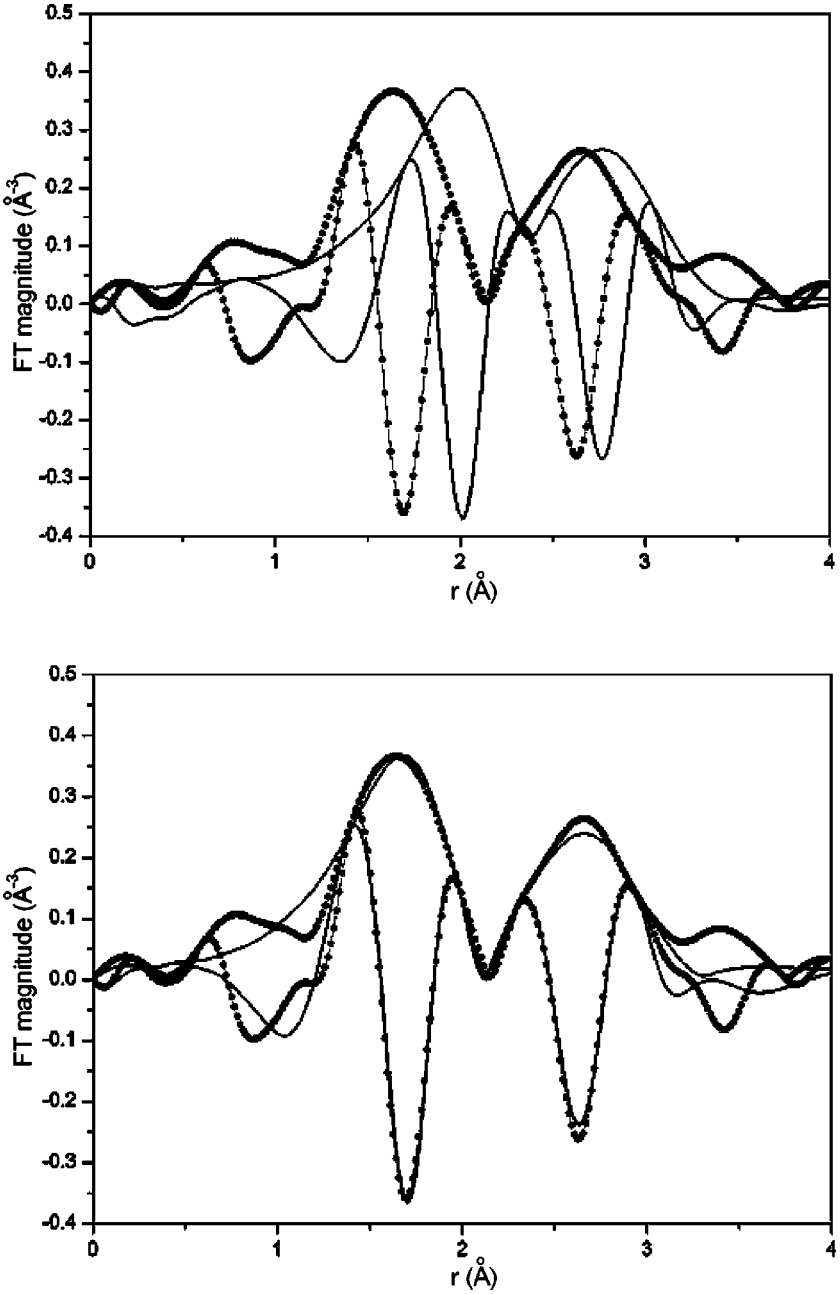

FIG. 2. Fourier transform of the Bi L_{III}-edge experimental spectrum of $Na_{0.5}Bi_{0.5}TiO_3$ (a) versus calculations using diffraction data; (b) with the results of the fit (the experimental spectrum is shown dotted and theoretical curves with solid lines).

values may be an indication of such static disorder.

The Bi L_{III}-XAFS Fourier transforms show a rather subtle dependence on the K concentration. As can be seen from Fig. 3, the positions of the Bi-O and Bi-Ti peaks do not change much in the whole concentration range. The slight increase of the peak intensities, which is observed as the potassium concentration grows, is probably the result of a more symmetrical nearest-neighbor environment of Bi atoms in K-rich samples. The Bi-O peak in all of the spectra has been successfully fitted with the same model as in pure NBT.

The refined structural parameters for several KNBT compositions are summarized in Table I. Correlations between ΔE_0 and R fitting parameters were moderate (about -0.7) and did not affect significantly the accuracy of the distance determination. It can be seen that the shortest Bi-O distances for all the compositions were found to be 2.22 Å, which is the typical value for Bi^{3+} oxides but which is 0.3 Å less than the distance derived from neutron diffraction for these compounds. This means that Bi is strongly displaced off-center in the oxygen polyhedron, and thus it forms short bonds of 2.22 Å with only several oxygen atoms out of 12 that form a Bi coordination polyhedron. The fit shows that the closest Bi-O shell includes about three atoms. Since no other peaks, which may correspond to Bi-O distances are observed we may suggest that these distances are too long and too widely spread to give a noticeable contribution to EXAFS signal. Bi-Ti distances vary within the range 3.22–3.24 Å depending on the composition, which are also less than values from the diffraction experiments. Although the fit to the data by only one Bi-Ti shell gives good results, a more complicated Ti radial atomic distribution around Bi cannot be ruled out. The coordination numbers and Debye-Waller factors show

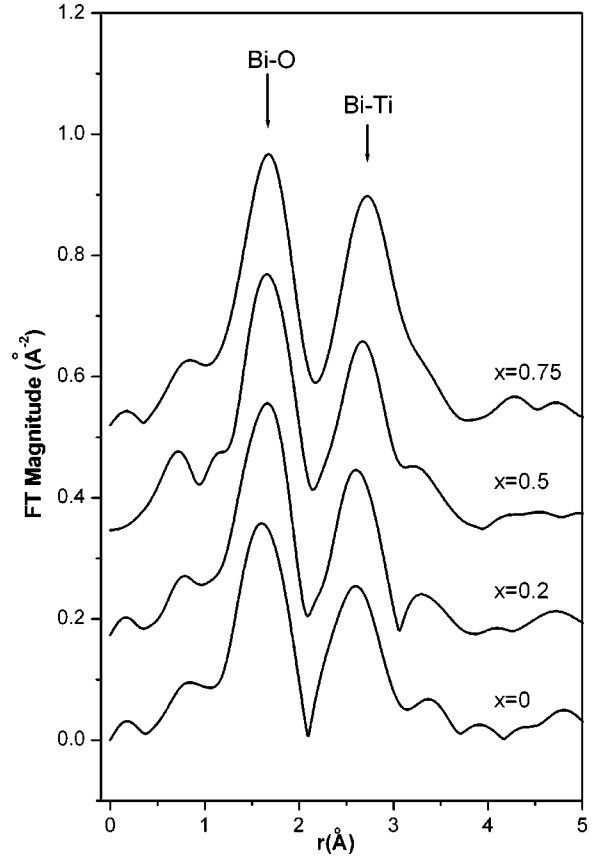

FIG. 3. The compositional dependence of the FT of Bi L_{III}-edge EXAFS of $(K_xNa_{1-x})_{0.5}Bi_{0.5}TiO_3$.

much stronger variation across the compositional range however the accuracy of determination of these values is low. It also should be taken into account that these parameters are strongly correlated and very sensitive to the non-Gaussian part of the radial atomic distribution and thus represent only "effective" values within the Gaussian approximation of the real atomic distribution, which may consist of several coordination shells with close radii. The refined σ^2 values for both shells decrease with increasing of K content which shows that in pure NBT Bi has a more distorted coordination with greater variation of Bi-O and Bi-Ti distances compared with K containing samples.

Short Bi-O bonds as observed by XAFS can be achieved in two ways: (1) by additional displacement of Bi along the polar direction with respect to the average structure and (2) by displacement of Bi atoms away from the polar axis in a plane orthogonal to the polar axis. In both cases this is likely to occur with statistical disorder. The values of off-center displacement of Bi which allow one to achieve consistency with XAFS data for these two models are estimated to be 0.65 and 0.7 Å, respectively, and thus the local dipole moment associated with Bi is much larger than has been suggested before. The Bi position within the oxygen polyhedron and the geometry of the Bi-O shortest bonds for the diffraction model and two possible models assuming additional Bi shifts are shown in Fig. 4. In the diffraction model all the shortest bonds have a planar configuration orthogonal to the polar axis and arise as a result of tilting of the oxygen octahedra. On the other hand, in the alternative models consistent with XAFS, Bi forms a pyramid with the nearest oxygen environment.

A valuable tool for a quick check of the plausibility of a structure is that of bond-valence sum calculations.[41–43] For the diffraction model bond valence sum (BVS) the value of the Bi cations is calculated to be 2.38.[15] It is therefore clear, that the model gives unsatisfactory coordination for the Bi atoms, as this suggests that they are severely underbonded in the symmetrical environment. On the other hand, for the modified models the Bi BVS is equal to 2.90 and 3.13, respectively, showing much more optimal bonding for the Bi cations.

Comparison of Bi-O distances for models (b) and (c) show that model (b) gives only four different Bi-O shells with three atoms at each while model (c) gives much broader distribution of Bi-O distances consisting of ten different shells with nine of them formed by only one atom. Thus the fact that no distant Bi-O shells are observed in the experiment favor the model (c).

Further diffraction and diffuse scattering studies aimed at improving upon the average structural models for KNBT are now in progress. A refinement[44] of the original neutron data[22] for the *R*3*c* phase of NBT gives a possible model (with goodness-of-fit, $\chi^2=1.05$) in which the Bi position of the original average structure is replaced by three Bi atoms each with one-third occupancy and displaced off the polar axis

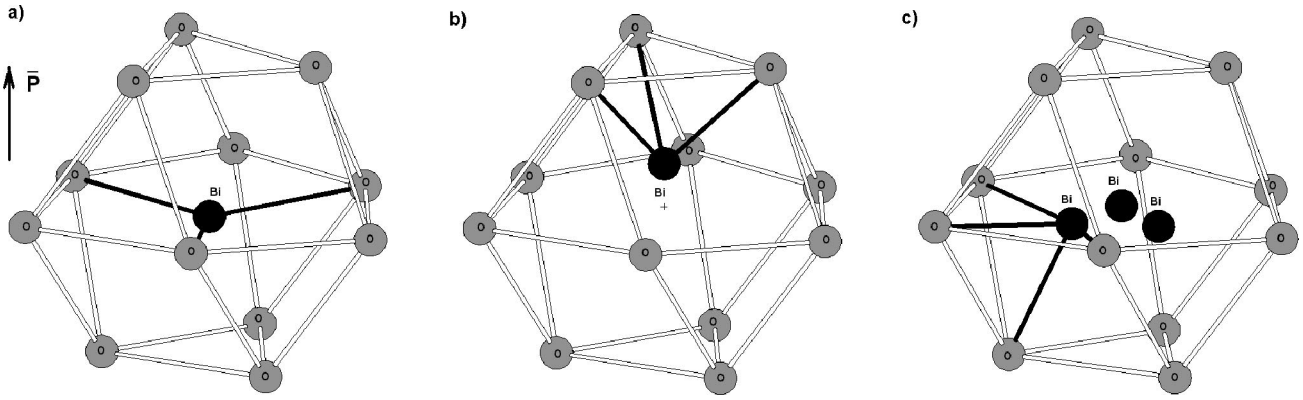

FIG. 4. Bi position within the oxygen polyhedron and the geometry of Bi-O shortest bonds; (a) the diffraction model, (b) Bi additionally displaced along the polar [111] direction, and (c) Bi atoms statistically disordered around the threefold axis.

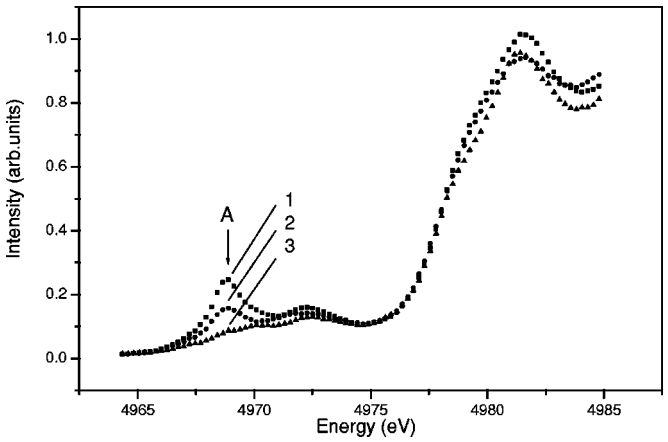

FIG. 5. The pre-edge part of the absorption spectra of $PbTiO_3$; (1) powder sample in the tetragonal phase (room temperature), (2) powder sample in the cubic phase (600 °C), and (3) single-crystal sample, tetragonal phase, and x-ray polarization vector orthogonal to the polar axis.

along the pseudocubic $[\bar{1}01]$ direction. This model is consistent with the diffraction data and immediately yields a Bi-O bond length of 2.223(8) Å, in agreement with the EXAFS study. Disorder of the oxygen atoms and an additional component of Bi displacement along the polar [111] axis yield from two to four neighbors at the short-bonded distance, depending upon the Bi displacements assumed, although it is not possible to discriminate between these different models using goodness-of-fit indicators in Rietveld refinement. However, it can be concluded that the rerefined diffraction data presently favor a local structure for Bi similar to model (c) of Fig. 4.

B. Ti *K*-XAFS

Absorption spectra provide two independent accurate tools for characterizing the Ti displacement in perovskites, namely pre-edge structure and EXAFS.

Pre-edge structure is a sensitive probe for detecting the deviations of transition metals from high-symmetry sites, as the amplitude of the peak in the absorption spectra located at energies just below the absorption edge of a transition element correlates with the displacement of the atom from a center of symmetry.[4,5] Theoretical calculations of the integrated intensity of the peak show that it is proportional to Δ^2, where Δ is the mean-square displacement of the absorbing atom. This provides a possibility for quantitative evaluation of the local structural distortions in perovskites.

The sensitivity of the pre-edge structure for off-center Ti displacements in the oxygen octahedron in perovskites can be illustrated by the absorption spectra of $PbTiO_3$ shown in Fig. 5. Spectra 1 and 2 were measured from a powder sample of $PbTiO_3$ at room temperature and at 600 °C, respectively, and thus correspond to tetragonal and cubic phases. We can see that in the tetragonal phase, the intensity of the pre-edge peak is much stronger than in the cubic phase. Spectrum 3 was taken at room temperature from a $PbTiO_3$ single crystal with the *c* axis oriented orthogonally to the x-ray polarization vector. In the latter case the Ti displacement along *c*, the polar axis, does not contribute to the pre-edge peak intensity while the other two components of the Ti displacement are close to zero. Thus we can see that, in this case, the pre-edge peak is not observed. These spectra were measured under the same experimental conditions as the spectra of the studied compounds and were used as reference spectra for quantitative determination of Ti off-center displacement in KNBT.

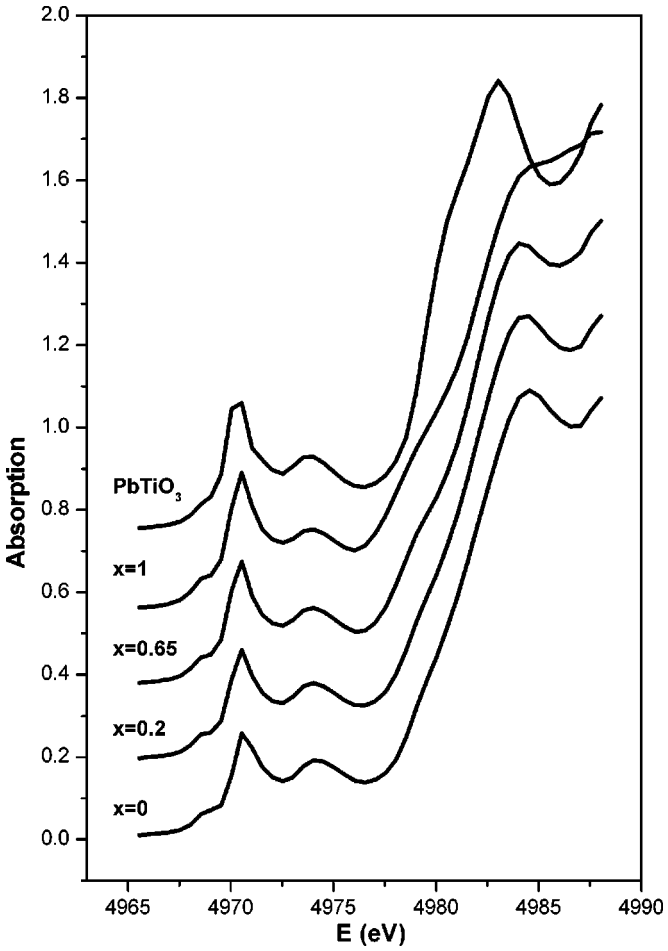

FIG. 6. The compositional dependence of the pre-edge structure of $(Na_{1-x}K_x)_{0.5}Bi_{0.5}TiO_3$ solid solution compared with the $PbTiO_3$ pre-edge structure.

The change of the pre-edge structure of KNBT crystals with composition is shown in Fig. 6 together with the $PbTiO_3$ pre-edge structure used as a reference. It can be seen that in pure KBT, the amplitude of the pre-edge peak is approximately the same as in $PbTiO_3$ and the integrated intensities of the peaks have very similar values. Thus the Ti displacement in KBT can be estimated to be equal to that in $PbTiO_3$, namely 0.25 Å. A gradual reduction of the pre-edge peak amplitude occurs as a result of substitution of K for Na. Estimates of the Ti displacement in pure NBT give a value 0.18 Å, which is larger than the value of 0.11 Å derived from the diffraction data.[15] The larger value of Ti displacement gives a slight improvement of Ti bond-valence sum compared with the diffraction model (3.96 vs 3.91). The reduction of the Ti displacement as a result of substitution is not dramatic and most likely is just a result of the reduction of the unit cell parameters.

We have also made a study of the changes of the NBT pre-edge structure with temperature. The transformations of the macroscopic symmetry in this compound occur as follows: Rhombohedral (220 °C)→mixed (rhombohedral +tetragonal) (320 °C)→tetragonal (560 °C)→cubic. The tetragonal phase was solved as a weakly polar phase in space group *P4bm*,[17] in which the Ti and Na/Bi displacements refined in opposite senses along the polar axis.

The polar nature of this phase was also confirmed by the observation of weak optical second harmonic generation[17] and piezoelectric signals.[26] The value of Ti off-center shift in this phase was determined to be about 0.06 Å. Thus a substantial decrease of Ti off-center displacement in the phase transition point should be observed. The cubic phase was refined as a paraelectric phase in space group $Pm\bar{3}m$, and, accordingly, the Ti displacement relative to the octahedron vanishes in this centrosymmetric structure. However, the pre-edge peak intensity does not show any temperature variations at all, as can be seen from Fig. 7, and even in the cubic phase there is no reduction of the Ti off-center shift. This result suggests that the symmetry of the high-temperature phase of the crystals is cubic only on a macroscopic scale, while the local distortions persist well above the phase transition point. The high symmetry emerges as a result of the averaging of spatial orientation of the low-symmetry units.

Our attempts to fit Ti *K*-EXAFS assuming either [111] or [100] Ti displacement were not successful for any of the measured patterns, which shows that the local Ti symmetry in all the phases of KNBT deviates from the average symmetry and thus Ti disorder should be seriously considered. The disorder however leads to a quite complicated radial atomic distribution around Ti, which makes it impossible to describe it quantitatively and to determine the direction of Ti off-center shift from powder EXAFS alone because of excessive number of the fitting parameters needed in the fit. Thus further refinement of Ti position will be possible through the use of polarized XAFS and diffraction studies which are in progress now.

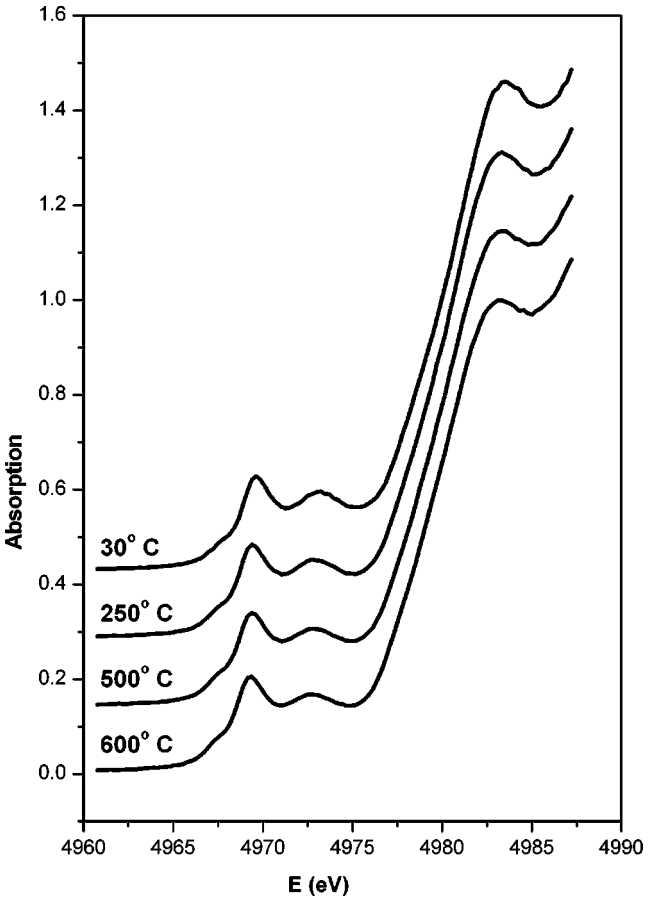

FIG. 7. The temperature dependence of the pre-edge structure at the Ti *K*-edge of $Na_{0.5}Bi_{0.5}TiO_3$.

IV. SUMMARY

As a result of this study of the local structure of KNBT crystals, significant local distortions of the ideal perovskite structure have been revealed which appear to be much greater than the average distortions obtained previously using diffraction techniques. The most likely reason for this disagreement is the presence of structural disorder, which can be difficult to determine from powder diffraction. The substitution of Na for K results in a larger Ti displacement, although the changes of the local structure are subtle. The changes of the macroscopic symmetry at the phase transitions in NBT crystal do not make any noticeable impact on the Ti environment. The results show that the relative atomic displacements are constant and thus a "displacive" mechanism is not involved and the phase transitions should be considered as primarily order disorder.

ACKNOWLEDGMENT

We are grateful to the Engineering and Physical Sciences Research Council (UK) for a grant enabling this work to be carried out.

[1] G. A. Samara, J. Phys.: Condens. Matter **15**, R367 (2003).
[2] R. Pirc and R. Blinc, Phys. Rev. B **60**, 13470 (1999).
[3] R. Fisch, Phys. Rev. B **67**, 094110 (2003).
[4] B. Ravel and E. A. Stern, Physica B **208&209**, 316 (1995).
[5] R. V. Vedrinskii, V. L. Kraizman, A. A. Novakovich, Ph. V. Demekhin, and S. V. Urazhdin, J. Phys.: Condens. Matter **10**, 9561 (1998).
[6] B. Ravel, E. A. Stern, Y. Yacobi, and F. Dogan, Jpn. J. Appl. Phys., Part 1 **32**, 782 (1993).
[7] B. Ravel, E. A. Stern, R. I. Vedrinskii, and V. Kraizman, Ferroelectrics **206–207**, 407 (1998).
[8] Y. Girshberg and Y. Yacoby, Solid State Commun. **103**, 425 (1997).
[9] V. A. Shuvaeva, K. Yanagi, K. Yagi, K. Sakaue, and H. Terauchi,

Solid State Commun. **106**, 335 (1998).
[10] V. A. Shuvaeva, Y. Azuma, K. Yagi, H. Terauchi, R. Vedrinski, V. Komarov, and H. Kasatani, Phys. Rev. B **62**, 2969 (2000).
[11] V. A. Shuvaeva, I. Pirog, Y. Azuma, K. Yagi, K. Sakaue, H. Terauchi, I. P. Raevskii, K. Zhuchkov, and M. Yu. Antipin, J. Phys.: Condens. Matter **15**, 2413 (2003).
[12] V. V. Ivanova, A. G. Kapyshev, Y. N. Venetsev, and G. S. Zhdanov, Izv. Akad. Nauk SSR Ser. Fiz. Mat. Nauk **24**, 354 (1962).
[13] G. A. Smolenskii, V. A. Isupov, A. I. Agranovskaya, and N. N. Krainik, Fiz. Tverd. Tela (Leningrad) **2**, 2982 (1960) [Sov. Phys. Solid State **2**, 2651 (1960)].
[14] J. A. Zvirgzds, P. P. Kapostins, J. V. Zvirgzde, and T. V. Kruzina, Ferroelectrics **40**, 75 (1982).
[15] G. O. Jones and P. A. Thomas, Acta Crystallogr., Sect. B: Struct. Sci. **58**, 168 (2002).
[16] S. B. Vakhrushev, B. G. Ivanitskii, B. E. Kvyatkovskii, A. N. Maistrenko, R. S. Malysheva, N. M. Okuneva, and N. N. Parfenov, Fiz. Tverd. Tela (Leningrad) **25**, 2613 (1983) [Sov. Phys. Solid State **25**, 1504 (1983)].
[17] G. O. Jones and P. A. Thomas, Acta Crystallogr., Sect. B: Struct. Sci. **56**, 426 (2000).
[18] T. V. Kruzina, V. V. Gene, V. A. Isupov, and E. V. Sinyakov, Kristallografiya **26**, 852 (1981) [Sov. Phys. Crystallogr. **26**, 482 (1981)].
[19] V. A. Isupov, I. P. Pronin, and T. V. Kruzina, Ferroelectr., Lett. Sect. **2**, 205 (1984).
[20] M. Geday, J. Kreisel, K. Roleder, and A. M. Glazer, J. Appl. Crystallogr. **33**, 909 (2000).
[21] T. V. Kruzina, V. M. Duda, and J. Suchanicz, Mater. Sci. Eng., B **87**, 48 (2001).
[22] G. O. Jones, J. Kreisel, and P. A. Thomas, Powder Diffr. **17**, 301 (2002).
[23] I. P. Pronin, N. N. Parfenova, N. V. Zaitseva, V. A. Isupov, and G. A. Smolenskii, Sov. Phys. Solid State **24**, 1060 (1982).
[24] V. A. Shuvaeva, A. M. Glazer, Q. Jiang, P. Thomas, D. Zekria, J. Kreisel, and M. A. Geday (unpublished).
[25] J. Kreisel, P. Bouvier, B. Dkhil, P. A. Thomas, A. M. Glazer, T. R. Welberry, B. Chaabane, and M. Mezouar, Phys. Rev. B **68**, 014113 (2003).
[26] K. Roleder, I. Franke, A. M. Glazer, P. A. Thomas, S. Miga, and J. Suchanicz, J. Phys.: Condens. Matter **14**, 5399 (2002).
[27] J.-R. Gomah-Pettry, S. Said, P. Marchet, and J.-P. Mercurio, J. Eur. Ceram. Soc. **24**, 1165 (2004).
[28] S. Said and J. P. Mercurio, J. Eur. Ceram. Soc. **21**, 1333 (2001).
[29] H. Nagata and T. Takenaka, J. Eur. Ceram. Soc. **21**, 1299 (2001).
[30] P. A. Thomas, J. Kreisel, A. M. Glazer, P. Bouvier, Q. Jiang, and R. Smith (unpublished).
[31] E. Prouzet, E. Husson, N. de Mathan, and A. Morell, J. Phys.: Condens. Matter **5**, 4889 (1993).
[32] C. Malibert, B. Dhil, J. M. Kiat, D. Durand, J. F. Berar, and A. Spasojevic-de Bire, J. Phys.: Condens. Matter **9**, 7485 (1997).
[33] K. S. Knight and K. Z. Baba-Kishi, Ferroelectrics **173**, 341 (1995).
[34] S. G. Zhukov, V. V. Chernyshev, L. A. Aslanov, S. B. Vakhrushev, and H. J. Schenk, J. Appl. Crystallogr. **28**, 385 (1995).
[35] K. V. Klementiev, *VIPER for Windows*, freeware: www.desy.de/~klmn/viper.html.
[36] K. V. Klementev, J. Phys. D **34**, 209 (2001).
[37] E. A. Stern, M. Newville, B. Ravel, Y. Yacoby, and D. Haskel, Physica B **209**, 117 (1995).
[38] M. Newville, P. Livins, Y. Yacoby, J. J. Rehr, and E. A. Stern, Phys. Rev. B **47**, 14 126 (1993).
[39] A. L. Ankudinov, B. Ravel, J. J. Rehr, and S. D. Conradson, Phys. Rev. B **58**, 7565 (1998).
[40] ICSD database: www.fiz-informationsdienste.de/en/DB/icsd/.
[41] G. Donnay and R. Allmann, Am. Mineral. **55**, 1003 (1970).
[42] I. D. Brown, Acta Crystallogr., Sect. B: Struct. Sci. **48**, 553 (1992).
[43] I. D. Brown, Acta Crystallogr., Sect. B: Struct. Sci. **53**, 381 (1997).
[44] P. A. Thomas (unpublished).